

# Viscous dissipation in steep capillary–gravity waves

By MICHAEL S. LONGUET-HIGGINS

Institute for Nonlinear Science, University of California, San Diego, La Jolla, CA 92093-0402, USA

(Received 11 November 1996 and in revised form 24 March 1997)

Some simple but exact general expressions are derived for the viscous stresses required at the surface of irrotational capillary–gravity waves of periodic or solitary type on deep water in order to maintain them in steady motion. These expressions are applied to nonlinear capillary waves, and to capillary–gravity waves of solitary type on deep water. In the case of pure capillary waves some algebraic expressions are found for the work done by the surface stresses, from which it is possible to infer the viscous rate of decay of free, nonlinear capillary waves.

Similar calculations are carried out for capillary–gravity waves of solitary type on deep water. It is shown that the limiting rate of decay of a solitary wave at low amplitudes is just twice that for linear, periodic waves. This is due to the spreading out of the wave envelope at low wave steepnesses. At large wave steepnesses the dissipation increases by an order of magnitude, owing to the sharply increased curvature in the wave troughs. The calculated rates of decay are in agreement with recent observations.

---

## 1. Introduction

Most work on the theory of capillary–gravity waves on deep water has assumed the fluid to be inviscid. With waves of very low amplitude or slope, and of sufficiently long wavelength the assumption can be justified; as Lamb (1932) has shown, the time-constant for the decay of low surface waves is about  $0.712\lambda^2$  s, where  $\lambda$  denotes the wavelength in cm. For gravity waves of length greater than a few centimetres this linear damping is relatively unimportant, but for capillary waves, say  $\lambda < 1$  cm, the damping becomes increasingly significant as  $\lambda$  diminishes. Moreover, nonlinear gravity waves with lengths between about 5 and 150 cm, which usually carry parasitic capillary waves on their forward slopes, are subject to much higher rates of decay for this very reason (Longuet-Higgins 1963).

Naturally occurring capillary waves, however, are frequently quite steep and nonlinear, especially parasitic capillaries. The solitary capillary–gravity waves predicted by Longuet-Higgins (1988, 1989) and confirmed by Vanden-Broeck & Dias (1992) have been found among wind-generated surface waves in the laboratory (Zhang 1995), sometimes with slopes approaching  $45^\circ$ . What is their expected rate of decay?

The present enquiry was prompted by a recent laboratory study of deep-water solitons (Longuet-Higgins & Zhang 1997) in which the decay of the solitons was measured experimentally. There has apparently been no theoretical calculation with which to compare the observations.

In contrast to shallow-water waves, where most of the dissipation comes from a

well-understood boundary layer at the bottom, in a deep-water wave when the surface stress vanishes and there is no meniscus, the bulk of the dissipation occurs throughout the fluid as ‘volume dissipation’. Even the presence of a thin vortical boundary layer does not change the total dissipation, to lowest order in  $k\delta$  where  $k$  is the wavenumber and  $\delta$  the boundary-layer thickness. (The validity of the boundary-layer theory for wavelengths down to 1 mm can be seen from table 2 of Longuet-Higgins 1992).

At first sight calculation of the volume dissipation appears to require the evaluation of a double integral over the entire body of the fluid. But an alternative approach was pointed out by Lamb (1932, §348) for linear waves. He argued that to maintain a steady wave in a viscous fluid certain stresses must be applied at the surface. Moreover in a steady state the total volume dissipation would be just equal to the work done by these virtual surface stresses against the particle motion at the surface. Using linear theory, he was thus able to calculate the total volume dissipation and hence the free rate of decay, to lowest order in  $k\delta$ . This was done only for linear waves, but it is evident that if we can find the surface stresses in nonlinear waves, and hence the work done against them, we can infer the total volume dissipation in that case also, at the expense of only one integration along the surface instead of a double integration throughout the volume.

To estimate the decay rate of a *free* nonlinear wave, a further assumption is necessary, namely that the nonlinear wave maintain its steady form approximately while decaying under the action of viscosity – an assumption that is plausible if the dissipation is sufficiently weak.

Such is the programme carried out in the present paper. In §2 we first derive some very simple expressions for the stresses  $\tau_{nn}$  and  $\tau_{ns}$  normal and tangential to the surface in terms of the local curvature  $\kappa$  and particle velocity  $q$  in a reference frame moving with the wave; see equation (2.8). It is assumed that the flow is irrotational, to lowest order. In §3 we calculate the total rate of working against the surface stresses (equation (3.9)). For steady waves either periodic in space or isolated as solitary waves, the expression simplifies remarkably, giving the very simple and useful formulae (3.10) and (3.11). The hodograph transformation which is convenient in subsequent work, is introduced in §4, and in §5 we check the formulae by showing how for linear waves the known rate of damping is recovered.

The first application to nonlinear waves is in §6, where the general formula (3.10) is applied to pure capillary waves. Here Crapper’s (1957) exact solution is found to lead directly to an explicit expression for the dissipation  $D$  which is algebraic in the amplitude parameter  $A$ ; see equation (6.16). Together with the known expressions for the kinetic and potential energies of a Crapper wave (which also are algebraic in the parameter  $A$ ) one can easily calculate the time-rate of decay as shown in figure 4, §7.

The second and main application of the general formulae is to solitary waves on deep water, as described in §§8 and 9. Here we are helped by the fact that for *steep* solitary waves the total energy  $E$  has already been calculated in Longuet-Higgins (1989) and that there exists a good approximation for the wave profile enabling us to evaluate analytically the dissipation  $D$  in steep waves (§8). On the other hand for *low* waves it is known that a solitary wave behaves as a wave packet whose width spreads out in inverse proportion to the wave amplitude (see Longuet-Higgins 1993; Akylas 1993). This enables us to provide satisfactory asymptotes to  $D$  and  $E$  at low wave amplitudes. As a result we can construct a theoretical curve for the time history of a decaying solitary wave (figure 8.). Noteworthy is the fact that at low steepnesses the maximum surface slope in a solitary wave decays at twice the rate for

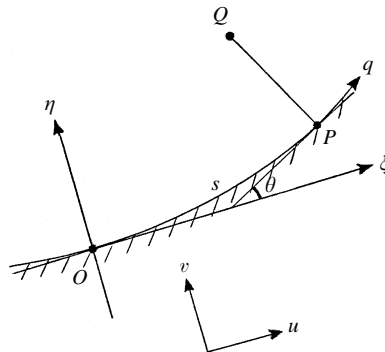


FIGURE 1. Definition of coordinates in the frame of reference moving with the phase speed  $c$ .

a linear, periodic wave. This is because the reduced energy has to be spread over an ever-widening horizontal distance.

In §10 the theory is compared with laboratory measurements and found to be in good agreement. A statement of the conclusions follows in §11.

**2. Surface stresses: general equations**

Consider a uniform, incompressible fluid in steady, two-dimensional irrotational motion, as in figure 1. Denote by  $s$  the distance along the surface from a fixed point  $O$  to a variable point  $P$  on the surface, and  $n$  the distance normal to the surface from  $P$  to an arbitrary point  $Q$  in the plane of motion.  $O\xi$  and  $O\eta$  are fixed rectangular axes at  $O$ , and  $\theta$  denotes the angle between  $O\xi$  and the tangent at  $P$ . Let  $q$  denote the particle velocity at  $P$ . Then the components  $(u, v)$  of the velocity in the fixed directions  $(O\xi, O\eta)$  are given by

$$u = q \cos \theta, \quad v = q \sin \theta. \tag{2.1}$$

The normal and tangential components of stress at  $O$  are given by

$$\tau_{nn} = -p + 2\mu \frac{\partial v}{\partial \eta}, \quad \tau_{ns} = \mu \left( \frac{\partial u}{\partial \eta} + \frac{\partial v}{\partial \xi} \right), \tag{2.2}$$

where  $p$  is the mean pressure and  $\mu$  is the coefficient of viscosity (see Lamb 1932, §326). At the free surface we shall suppose  $p = -T\kappa$  where  $\kappa$  is the local curvature and  $T$  the surface tension. Also since the flow is non-divergent and irrotational

$$\frac{\partial u}{\partial \xi} + \frac{\partial v}{\partial \eta} = 0, \quad \frac{\partial u}{\partial \eta} - \frac{\partial v}{\partial \xi} = 0. \tag{2.3}$$

Hence we have

$$\tau_{nn} = T\kappa - 2\mu \frac{\partial u}{\partial \xi}, \quad \tau_{ns} = 2\mu \frac{\partial v}{\partial \xi}, \tag{2.4}$$

where

$$\frac{\partial}{\partial \xi} = \cos \theta \frac{\partial}{\partial s} + \sin \theta \frac{\partial}{\partial n}. \tag{2.5}$$

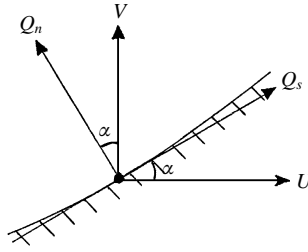


FIGURE 2. Definition of velocity vectors in the stationary frame of reference.

On substituting for  $u$  and  $v$  from equation (2.1) and carrying out the differentiation, then setting  $\theta = 0$ , we have

$$\frac{\partial u}{\partial \xi} = \frac{\partial}{\partial s}(q \cos \theta) = \frac{\partial q}{\partial s}, \quad \frac{\partial v}{\partial \xi} = \frac{\partial}{\partial s}(q \sin \theta) = q \frac{\partial \theta}{\partial s} = \kappa q \quad (2.6)$$

since

$$\kappa = \frac{\partial \theta}{\partial s}. \quad (2.7)$$

Hence finally from (2.4)

$$\tau_{nn} = T\kappa - 2\mu \frac{\partial q}{\partial s}, \quad \tau_{ns} = 2\mu\kappa q. \quad (2.8)$$

These equations express the stresses in terms of the local velocity  $q$  and the local geometry of the surface, and so are valid at all points. However  $q$  must be the velocity in a reference frame in which the flow is steady.

### 3. Work done against surface stresses

Consider any steady surface wave travelling to the left with speed  $c$ , as in figure 2. Let  $U$  and  $V$  denote the horizontal and vertical components of velocity, in this (stationary) surface frame. These are related to the steady velocity  $q$  seen in a frame moving with speed  $c$  to the left by

$$U = q \cos \alpha - c, \quad V = q \sin \alpha, \quad (3.1)$$

where  $\alpha$  is the local angle between the surface and the horizontal. Now in the stationary reference frame the local components of velocity tangential and normal to the surface are given by

$$Q_s = U \cos \alpha + V \sin \alpha, \quad Q_n = -U \sin \alpha + V \cos \alpha, \quad (3.2)$$

or on substitution from (3.1)

$$Q_s = q - c \cos \alpha, \quad Q_n = c \sin \alpha. \quad (3.3)$$

Hence the rate of working  $W$  of these velocities against the surface stresses, which is given by

$$W = Q_n \tau_{nn} + Q_s \tau_{ns}, \quad (3.4)$$

becomes

$$W = 2\mu\kappa q^2 + cT\kappa \sin \alpha - 2\mu c \left( \frac{\partial q}{\partial s} \sin \alpha + \kappa q \cos \alpha \right) \quad (3.5)$$

per unit distance  $s$  along the surface. Now since  $\kappa = \partial\alpha/\partial s$  the second term can be written as

$$-\frac{\partial}{\partial s}(cT \cos \alpha) \tag{3.6}$$

while the two bracketed terms in (3.5) can be written

$$\frac{\partial}{\partial s}(q \sin \alpha). \tag{3.7}$$

Therefore if we define

$$D = \int_{s_1}^{s_2} W ds \tag{3.8}$$

as the total rate of working against the surface stresses we find from (3.5)

$$D = \int_{s_1}^{s_2} 2\mu\kappa q^2 ds - c[T \cos \alpha + 2\mu q \sin \alpha]_1^2. \tag{3.9}$$

Two special cases of this result are of particular interest. The first is when the surface waves are periodic in the  $x$ -direction. Then if the integration is taken over an integral number of wavelengths the last two terms of equation (3.5) vanish by the periodicity and we obtain

$$D = 2\mu \int_{s_1}^{s_2} \kappa q^2 ds. \tag{3.10}$$

Consider the mass of fluid contained between two vertical planes  $x = \text{constant}$  spaced one wavelength apart. The net rate of working on the fluid by stresses across the vertical boundaries is zero, by the periodicity. The work done at infinite depth is negligible, since the motion vanishes exponentially. Therefore the only work done is represented by equation (3.10), and in a steady state  $D$  must be equal to the total rate of dissipation of energy in the fluid.

The second case of interest is when the motion is a progressive solitary wave. Then if  $s_1$  and  $s_2$  are taken as  $-\infty$  and  $\infty$  respectively, the same terms also vanish and we obtain

$$D = 2\mu \int_{-\infty}^{\infty} \kappa q^2 ds. \tag{3.11}$$

Now in a solitary wave, the fluid velocity vanishes like  $1/r^2$  as the distance  $r = (x^2 + y^2)^{1/2}$  tends to infinity (see Longuet-Higgins 1989). Hence the work done by the stresses at infinity is negligible, and  $D$ , as given by equation (3.11), must be equal to the total rate of dissipation throughout the fluid.

It is interesting to compare equation (3.10) with an integral expression for the dissipation given by Lamb (1932, §329 (13)) namely

$$D = \mu \int \frac{\partial q^2}{\partial n} ds \tag{3.12}$$

where  $n$  denotes distance normal to the surface. This can easily be derived from equation (3.10) by noting that in an irrotational flow the normal to a streamline is locally an equipotential surface. Thus if we have two adjacent streamlines  $\phi$  and  $\phi + d\phi$ , then

$$0 = \frac{\partial}{\partial n}(d\phi) = \frac{\partial}{\partial n}(q ds) = \frac{\partial q}{\partial n} ds - q \kappa ds \tag{3.13}$$

since  $\partial(ds)/\partial n = -\kappa ds$ . Hence  $\kappa q = \partial q/\partial n$ , yielding (3.12). On the other hand

equation (3.10) is more advantageous for calculations, since it relates the dissipation to quantities evaluated at the free surface, rather than to a normal derivative.

#### 4. Hodograph transformation

It is often convenient to introduce the variable

$$\beta = \ln(q/c) \quad (4.1)$$

so that

$$q = ce^\beta \quad (4.2)$$

and

$$(U + c) - iV = ce^{\beta - i\alpha}. \quad (4.3)$$

Thus  $(\alpha + i\beta)$  is an analytic function of the velocity potential  $w = \phi + i\psi$ . Since  $d\phi/ds = q$  we have also

$$\kappa = \frac{d\alpha}{ds} = q \frac{d\alpha}{d\phi} = ce^\beta \frac{d\alpha}{d\phi}. \quad (4.4)$$

Hence

$$\int \kappa q^2 ds = \int q^2 d\alpha = c^2 \int e^{2\beta} d\alpha \quad (4.5)$$

and from §3

$$D = 2\mu c^2 \int e^{2\beta} d\alpha. \quad (4.6)$$

For periodic waves, since  $\int d\alpha = 0$  over one wavelength we have also

$$D = 2\mu c^2 \int (e^{2\beta} - 1) d\alpha. \quad (4.7)$$

#### 5. Linear surface waves

We may check the above analysis against the well-known linear theory of damped surface waves (e.g. Lamb 1932, §348). For a given surface elevation

$$\eta = a \cos k(x + ct) \quad (5.1)$$

we have

$$\alpha = \eta_x = -ak \sin k(x + ct) \quad (5.2)$$

Also

$$\phi = cx - ace^{ky} \sin k(x + ct). \quad (5.3)$$

and hence at the surface

$$q^2 = \phi_x^2 + \phi_y^2 = c^2(1 - 2ak \cos k(x + ct)) \quad (5.4)$$

to first order in  $ak$ , so

$$\beta = -ak \cos k(x + ct). \quad (5.5)$$

For linear waves, equation (4.7) reduces to

$$D = 4\mu c^2 \int \beta d\alpha \quad (5.6)$$

where the integral is to be taken over one wavelength  $L = 2\pi/k$ . This gives

$$D = 2L\mu c^2 a^2 k^3 = 4\pi\mu c^2 a^2 k^2 \quad (5.7)$$

for the total rate of dissipation. The mean rate of dissipation  $D'$  per unit horizontal distance is given by

$$D' = D/L = 2\mu c^2 a^2 k^3. \quad (5.8)$$

But the mean energy per unit horizontal distance is

$$E = \frac{1}{2}a^2(g + Tk^2) = \frac{1}{2}a^2c^2k \quad (5.9)$$

(the density being taken as unity). Thus

$$\frac{D'}{E} = 4vk^2 \quad (5.10)$$

where  $v$  is the kinematic viscosity, and

$$\frac{1}{a} \frac{da}{dt} = \frac{1}{2E} \frac{dE}{dt} = -\frac{D'}{2E} = -2vk^2 \quad (5.11)$$

as in Lamb (1932, p. 624).

## 6. Nonlinear capillary waves

The formulae of §§2–4 being fully applicable to nonlinear waves, we shall now apply them to the exact solution for pure capillary waves found by Crapper (1957).

If we choose units of length and time so that the phase speed  $c$  and wavenumber  $k$  are 1 and 2 respectively, Crapper's solution can be written

$$z = w - \tan w \quad (6.1)$$

where  $z = x + iy$  and  $w = \phi + i\psi$ , in a reference frame moving to the left with velocity  $-c$ . Any streamline  $\psi = \psi_0$  is a line of constant pressure and may be chosen as the free surface, so that we have a family of waves specified by the parameter

$$A = e^{-2\psi_0} \quad (6.2)$$

in the range  $0 < A < 0.4547$ , that is  $\infty > \psi_0 > 0.3941$ . The maximum angle of slope of the free surface is related to  $A$  by

$$\alpha_{\max} = 4 \tan^{-1} A \quad (6.3)$$

(see the Appendix) and the phase speed  $c$  is given by

$$c^2 = \frac{1 - A^2}{1 + A^2} Tk. \quad (6.4)$$

The potential and kinetic energies per horizontal distance are found to be

$$\text{PE} = \frac{4A^2}{1 - A^2} T, \quad \text{KE} = \frac{4A^2}{1 - A^4} T \quad (6.5)$$

(see Hogan 1979) so the total energy density is

$$E = \frac{4A^2(2 + A^2)}{1 - A^4} T. \quad (6.6)$$

Our task is to evaluate the surface integral

$$\frac{D}{2\mu} = \int \kappa q^2 ds = \int \kappa q d\phi, \quad (6.7)$$

the integral being taken over one wavelength  $L$ , for example  $0 < \phi < \pi$ . Note that from the boundary condition

$$\frac{1}{2}q^2 - T\kappa = \text{constant} = \frac{1}{2} \quad (6.8)$$

we have

$$q^2 = 1 + 2T\kappa \quad (6.9)$$

and so from (6.7)

$$\frac{D}{2\mu} = \int (\kappa + 2T\kappa^2) ds = 2T \int \kappa^2 ds \quad (6.10)$$

since  $\int \kappa ds$  vanishes by the periodicity. However it is easier to apply (6.7) directly.

Now from equation (6.1) we have

$$\frac{dz}{dw} = 1 - \sec^2 w = -\tan^2 w \quad (6.11)$$

and so

$$q = \left| \frac{dw}{dz} \right| = \cot w \cot w^* \quad (6.12)$$

where a star denotes the complex conjugate. The surface curvature  $\kappa$  is given by

$$\kappa = \frac{\cos 2\phi \sinh 2\psi_0}{\sin^2 w \sin^2 w^*} \quad (6.13)$$

(Longuet-Higgins 1988). Hence writing  $\zeta = e^{2i\phi}$  we have

$$\kappa q = 4A(1 - A^2) \frac{\zeta(\zeta^2 + 1)(A\zeta + 1)(A + \zeta)}{(A\zeta - 1)^3(A - \zeta)^3}. \quad (6.14)$$

Since  $d\phi = d\zeta/(2i\zeta)$  equation (6.7) becomes

$$\frac{D}{2\mu} = 2iA(1 - A^2) \oint \frac{(\zeta^2 + 1)(A\zeta + 1)(A + \zeta)}{(A\zeta - 1)^3(\zeta - A)^3} d\zeta, \quad (6.15)$$

the integral being taken round the circle  $|z| = 1$ . Since  $|A| < 1$  the integrand has just one pole within the unit circle, namely at  $\zeta = A$ , and on taking  $2\pi i$  times the residue at this point<sup>†</sup> we obtain

$$\frac{D}{\mu c^2} = 64\pi \frac{A^6 + 4A^4 + A^2}{(1 - A^2)^4} \quad (6.16)$$

since  $c^2 = 1$ . Each side is now dimensionless. But  $\lambda = 2\pi/k$ , so we may use equation (6.4) to write the mean dissipation  $D' = D/\lambda$  as

$$D' = 32 \frac{A^6 + 4A^4 + A^2}{(1 + A^2)(1 - A^2)^3} \mu k^2 T. \quad (6.17)$$

The above result will be found, at length, to agree with an expression for the mean dissipation derived by Crapper (1970, equation (21)) after allowing for a change in

<sup>†</sup> That is, on replacing  $\zeta$  by  $(A + \epsilon)$  in the integrand, expanding in powers of  $\epsilon$ , and taking  $2\pi i$  times the coefficient of  $\epsilon^{-1}$ .



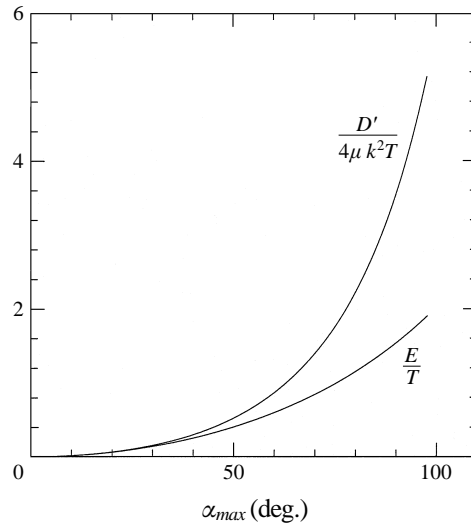


FIGURE 3. The scaled rate of dissipation  $D'$  and the energy density  $E$  for capillary waves as functions of the parameter  $\alpha_{max}$ .

notation. Crapper's derivation was based on Lamb's expression for  $D$ , equation (3.12) above.

Note that when  $A \ll 1$  equation (6.17) reduces to

$$D' \doteq 32A^2 \mu k^2 T. \tag{6.18}$$

But from (6.6) the total energy density  $E$  is

$$E \doteq 8A^2 T \tag{6.19}$$

in the limit. Hence

$$D'/E \doteq 4\nu k^2 \tag{6.20}$$

in agreement with equation (5.10).

In figure 3 the scaled rate of dissipation  $D'/4\mu k^2 T$  is plotted against  $\alpha_{max}$  (see equation (6.3)). The scaled energy density  $E/T$  is shown for comparison. It will be seen that for low values of  $\alpha_{max}$  the two curves touch, but at high values of  $\alpha_{max}$  the dissipation increases much more rapidly than the energy density. This behaviour will be further discussed in §10.

### 7. Viscous decay of a free wave

To follow the evolution of a surface wave which is free to decay on its own by viscous dissipation it is plausible to assume that, if the rate of decay is sufficiently slow, the wave motion at any given time is approximately that of a steady wave of the same amplitude. With linear sinusoidal waves, this can be easily justified. However if the waves are nonlinear, the validity of the assumption is less clear. Indeed it cannot possibly be exactly true, as we can show. For, consider a uniform irrotational wave train of finite amplitude  $a$ . This is associated with a horizontal momentum

$$M = E/c \doteq \frac{1}{2} a^2 kc \tag{7.1}$$

per unit distance. As the amplitude decays, this momentum is converted into a surface current, the vorticity so generated being diffused downwards from the free surface as described in Longuet-Higgins (1969). The depth to which the current penetrates is of order  $(\nu t)^{1/2}$ , where  $t$  denotes the elapsed time since the wave began to decay. Hence the time take for the vorticity to penetrate to a depth of order  $k^{-1}$  is of order  $1/(\nu k^2)$ , which is comparable to the natural decay time of the waves. Thus when the wave has reached some lower amplitude  $a'$  less than the starting amplitude  $a$ , it is propagated on a shearing current – the remnant of part of the momentum from the original wave. Hence the wave is no longer irrotational as assumed in our analysis.

The coupling between a surface wave and a second-order shearing current is, however, weak, as was shown by Dubreil-Jacotin (1934).

In addition we must bear in mind that the viscous boundary layer at the free surface is not of uniform thickness (see Longuet-Higgins 1969, 1992). Consequently, there are additional normal stresses on the fluid in the interior which could result in the generation of higher harmonics in the potential flow as the wave decays. Possibly these can be accommodated in a quasi-steady solution, but this is a question for future investigation.

In spite of these remarks it is nevertheless legitimate to assume as an approximation that in slowly decaying waves, at least, the wave is in a quasi-steady state which is given approximately by the irrotational solution described in §6.

Accordingly we assume here that, in a freely decaying wave of uniform amplitude,

$$\frac{dE}{dt} = -D' \quad (7.2)$$

where  $E$  and  $D'$  refer to the irrotational solutions. From (7.2) it follows that

$$t = - \int \frac{dE}{D'}. \quad (7.3)$$

In pure capillary waves, for example, we have on substitution from equations (6.6) and (6.17)

$$\nu k^2 t = \frac{1}{8} \int_A^{A_0} \frac{(1+A^2)(1-A^2)^3}{A^6 + 4A^4 + A^2} d \left( \frac{2A^2 + A^4}{1-A^4} \right) \quad (7.4)$$

where  $A_0$  denotes the values of  $A$  at the starting time  $t = 0$ . This can be simplified to

$$\nu k^2 t = \frac{1}{2} \int_A^{A_0} \frac{1-A^6}{1+5A^2+5A^4+A^6} \frac{dA}{A}. \quad (7.5)$$

The above integral may easily be evaluated numerically to give  $A$  as a function of  $t$ . In figure 4(a) the maximum slope  $\alpha_{max}$  (see equation (6.3)) is plotted as a function of the dimensionless time  $\nu k^2 t$ . From figure 4(b), which shows the logarithm of  $\alpha_{max}$  plotted similarly, it can be seen that the proportional rate of decay of  $\alpha_{max}$  is in this case nearly a constant over the whole range. We may say that the sharp rate of increase in the dissipation  $D$  at high wave slopes has been partly compensated by the rapid increase in the energy density  $E$ .

As pointed out by a referee, the integral in equation (7.5) can also be evaluated by partial fractions to yield

$$\nu k^2 t = \frac{1}{8} \ln \frac{(1+4A^2+A^4)^3}{(1+A^2)^2 A^4} - C \quad (7.6)$$

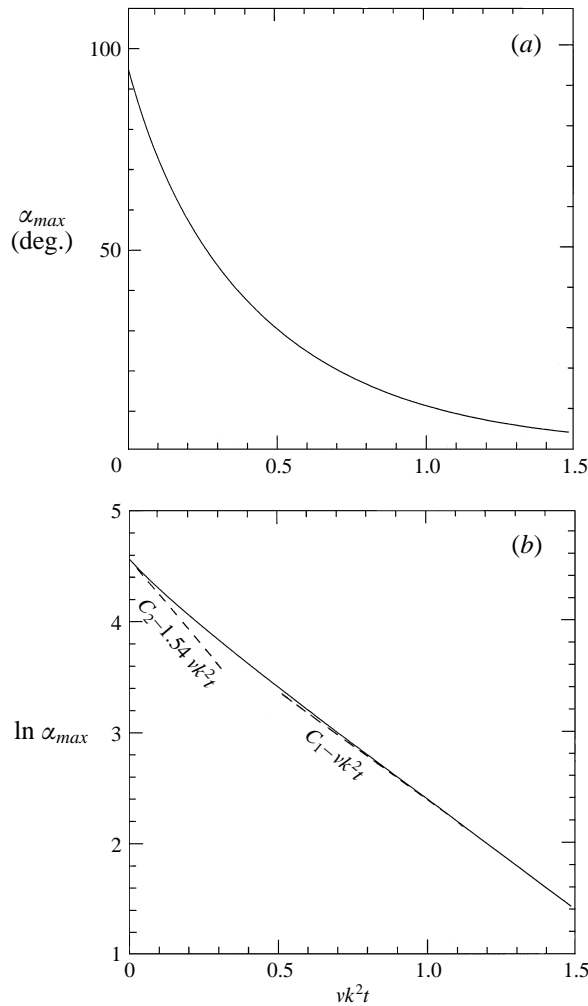


FIGURE 4. Time-history of the maximum surface slope in pure capillary waves decaying under viscosity. (a)  $\alpha_{max}$ , (b)  $\ln \alpha_{max}$ .

where  $C$  is a constant of integration. Choosing  $t = 0$  when  $A = 0.4547$  (see §6) gives us

$$C = 0.5818. \tag{7.7}$$

Let  $\bar{\alpha} = \frac{1}{2}\alpha_{max}$ , so that  $A = \tan \frac{1}{2}\bar{\alpha}$  by equation (6.3). Then equation (7.6) can be written in the form

$$e^{8vk^2t} = \frac{2\gamma^4(2 + \sin^2 \bar{\alpha})^3}{\sin^4 \bar{\alpha}} \tag{7.8}$$

where  $\gamma = e^{-2C} = 0.3124$ . Being effectively a cubic equation for  $\sin^2 \bar{\alpha}$  in terms of  $\exp(8vk^2t)$ , equation (7.8) may be solved explicitly for  $\sin^2 \bar{\alpha}$ , giving  $\alpha_{max}$  as a function of the time  $t$ . The result agrees with figure 4(a).

When  $\bar{\alpha}$  is small equation (7.8) yields, to a first approximation,

$$\sin \bar{\alpha} = 2\gamma e^{-2vk^2t}. \tag{7.9}$$

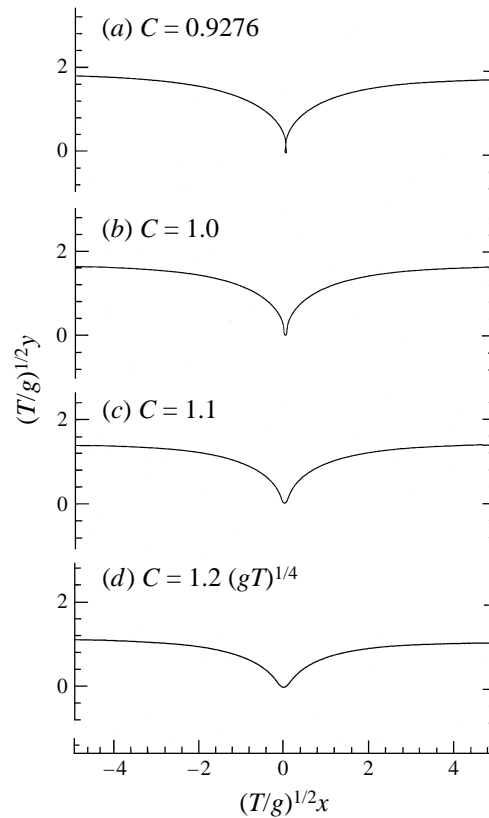


FIGURE 5. Approximate profiles of steep solitary waves as given by equation (8.2).  $C$  denotes the normalized phase speed  $c/(gT)^{1/4}$ . For maximum slopes, see table 1.

Hence

$$\alpha_{max} = \gamma e^{-2\nu k^2 t}, \quad (7.10)$$

which is in agreement with equation (5.11) and yields in addition the constant of proportionality.

## 8. Solitary waves on deep water

We shall now apply the general formulae of §4 to capillary-gravity solitary waves on deep water (see Longuet-Higgins 1989, 1992). For these waves there are no exact expressions as for pure capillary waves, but good approximations have been shown to exist in two cases: very steep solitary waves (Longuet-Higgins 1989), and solitary waves of very small steepness (Longuet-Higgins 1993; Akylas 1993). In both cases we can derive (approximate) closed expressions for the energy dissipation.

It is convenient in this Section to take units of length and time so that

$$g = 1, \quad T = 1. \quad (8.1)$$

For very steep waves, that is to say with a maximum slope exceeding about  $45^\circ$ , an approximation to the particle velocity at the free surface (relative to a frame moving

$c$	$\alpha_{max}$		PE	KE	$E$	$D/\mu$	$q_0$
	(rad.)	(deg.)					
0.9276	1.712	98.1	2.066	1.294	3.360	549.8	11.83
0.950	1.652	94.7	2.004	1.294	3.298	451.2	10.83
1.000	1.514	87.7	1.853	1.275	3.128	289.4	8.90
1.050	1.371	78.6	1.681	1.225	2.906	184.2	7.34
1.100	1.224	70.1	1.489	1.143	2.632	116.3	6.08
1.150	1.072	61.4	1.280	1.031	2.311	71.7	5.03
1.200	0.917	52.5	1.056	0.890	1.946	42.8	4.17
1.414	0.000	00.0	0.000	0.000	0.000	00.0	1.00

TABLE 1. Parameters for a solitary wave on deep water.

with speed  $c$  to the left) is given by the simple expressions

$$\alpha = B \frac{2\lambda}{(1 + \lambda^2)^2}, \quad \beta = B \frac{1 - \lambda^2}{(1 + \lambda^2)^2} \quad (8.2)$$

where  $B$  is a parameter and  $\lambda = \phi/c$ ; see Longuet-Higgins (1989, equation (4.2)). From these and from the Bernoulli relation

$$y = -\frac{1}{2}q^2 + T\kappa + \text{const.} \quad (8.3)$$

we may plot the profile of the free surface for a given value of the parameter  $B$ ; see figure 5. From (8.2) it can be seen that for each value of  $B$  the surface slope  $\alpha$  has a maximum value when  $\lambda^2 = 1/3$ , giving

$$\alpha_{max} = \frac{\sqrt{27}}{8} B = 0.6495. \quad (8.4)$$

In the limiting case  $B = 2.637$ , corresponding to  $\alpha_{max} = 98.1^\circ$ , the surface bends over and encloses a 'bubble of air', as in a pure capillary wave of maximum steepness (see §5). The phase speed of this wave is  $c = 0.9276 (gT)^{1/4}$ , see table 1. In general the surface profiles of the waves in figure 5, up to about  $c = 1.2$ ,  $\alpha_{max} = 43.6^\circ$ ,  $B = 1.172$ , closely resemble the exact profiles shown in figure 3 of Longuet-Higgins (1989). The chief discrepancy is in the outer parts of the waves, where the exact profiles approach the level at infinity from slightly above whereas in figure 5 they approach from slightly below. However, the curvature being small in these parts of the wave, the estimated dissipation is only very slightly affected.

On substituting in the general formula (4.7) we find for the total energy dissipation

$$D = 2\mu c^2 F(B) \quad (8.5)$$

where

$$F(B) = 2B \int_{-\infty}^{\infty} \frac{1 - 3\lambda^2}{(1 + \lambda^2)^3} \left[ \exp \left\{ \frac{2B(1 - \lambda^2)}{(1 + \lambda^2)^2} \right\} - 1 \right] d\lambda, \quad (8.6)$$

It is straightforward to evaluate the integral numerically. As a useful check we have when  $B \ll 1$

$$F(B) \sim 4B^2 \int_{-\infty}^{\infty} \frac{(1 - 3\lambda^2)(1 - \lambda^2)}{(1 + \lambda^2)^5} d\lambda = \frac{3\pi}{4} B^2. \quad (8.7)$$

In equation (8.5) the phase speed  $c$  is also a function of  $\alpha_{max}$ ; see table 1. Using the precisely calculated values of  $B$  given by equation (8.4) and table 1 we have plotted

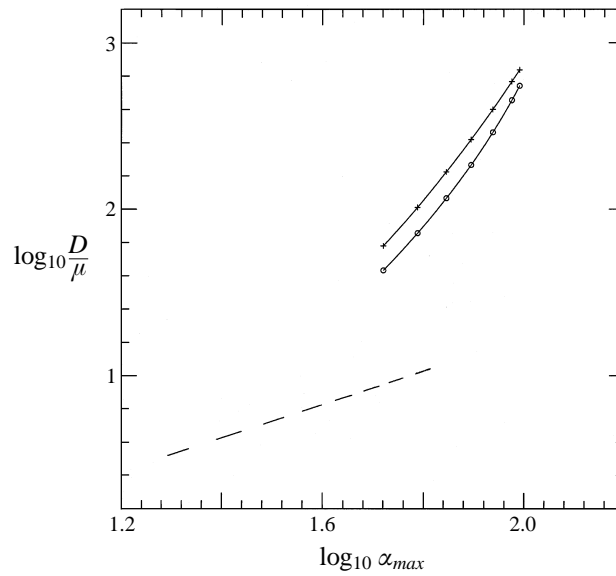


FIGURE 6. Rate of viscous dissipation of energy in a solitary wave as a function of the maximum slope  $\alpha_{max}$  (measured in degrees). Curves with crosses: from equation (8.6). Curves with circles: computed from equation (3.11) using the accurate numerical solution given in Longuet-Higgins (1989). Dashed line: asymptote from equation (9.9).

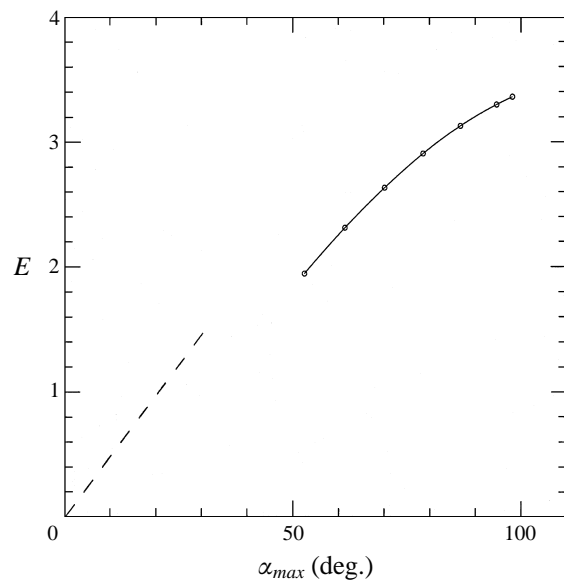


FIGURE 7. Total energy  $E$  of a solitary wave as a function of the maximum surface slope  $\alpha_{max}$ . Plotted points: computed values from Longuet-Higgins (1989). Dashed line: asymptote from equation (9.7).

in figure 6 the function  $D/\mu$  against  $\alpha_{max}$  (upper curve). It will be seen that there is an extremely sharp increase in  $D$  towards the higher values of  $\alpha_{max}$ .

To verify this sharp increase, we resort to the exact numerical calculation of solitary wave profiles given in Longuet-Higgins (1989) and evaluate the integral (3.11) numerically. The results are shown in table 1 and by the lower curve (plotted with

circles) in figure 6. It will be seen that the trends of the two curves are similar. Proportionally they differ by 25% to 40%.

The straight dashed line in the lower part of figure 6 represents an asymptote which will be derived below in §9.

For comparison we show in figure 7 the total energy  $E$  as a function of  $\alpha_{max}$  which was calculated numerically in Longuet-Higgins (1989). The values used are shown in table 1. The values are considered accurate down to  $\alpha_{max} = 52^\circ$ . The dashed curve in figure 7 represents an asymptote for low values of  $\alpha_{max}$  which will now be derived.

**9. Solitary waves: the low-amplitude limit**

It has been shown (Longuet-Higgins 1993; Akylas 1993) that in the limit of low wave steepness a solitary capillary gravity wave on deep water takes the form of a *wave packet* in which the surface elevation  $\eta$  is given to order  $\epsilon^3$  by

$$\eta = \frac{2\epsilon a\omega}{g + Tk^2} \cos(kx + \omega t - \epsilon^2 t) \operatorname{sech} [b\epsilon(x + c_g t)] \tag{9.1}$$

where  $k$  and  $\omega$  are the wavenumber and frequency of the carrier wave. Also

$$a^2 = \frac{16}{11} \omega, \quad b^2 = 2\omega \tag{9.2}$$

and  $c_g$  denotes the group velocity. Thus, as the amplitude parameter  $\epsilon$  diminishes, the width of the envelope increases as  $\epsilon^{-1}$ . The waves are steady with respect to the envelope if  $c = c_g$  which implies  $k = 1, \omega = \sqrt{2}$ , in units where  $g = T = 1$ . Hence to lowest order in  $\epsilon$  equation (9.1) can be written

$$\eta = \sqrt{2}a\epsilon \cos x \operatorname{sech}(b\epsilon x) \tag{9.3}$$

at time  $t = 0$ , and

$$\alpha_{max} = \sqrt{2} a\epsilon = \frac{4 \times 2^{3/4}}{\sqrt{11}} \epsilon. \tag{9.4}$$

The total energy  $E$  is given by

$$E = \frac{1}{2} \left( \frac{g}{k^2} + T \right) \alpha_{max}^2 \int_{-\infty}^{\infty} \operatorname{sech}^2(b\epsilon x) dx. \tag{9.5}$$

to lowest order, that is

$$E = \frac{2\alpha_{max}^2}{b\epsilon} = \frac{4a^2\epsilon^2}{b\epsilon} = \frac{32 \times 2^{3/4}}{11} \epsilon \tag{9.6}$$

or from equation (9.4)

$$E = \frac{8}{\sqrt{11}} \alpha_{max} = 2.412 \alpha_{max}. \tag{9.7}$$

It is notable that  $E$  is proportional to  $\alpha_{max}$  and not  $\alpha_{max}^2$ .

As in the linear theory (§5) the total dissipation  $D$  is given by

$$D = 4\nu k^2 E \tag{9.8}$$

to lowest order in  $\epsilon$ , that is to say

$$D = \frac{32}{\sqrt{11}} \nu k^2 \alpha_{max} = 9.648 \nu \alpha_{max}. \tag{9.9}$$

The two asymptotes (9.7) and (9.9) are shown by the dashed lines on figures 7 and 6 respectively.

From the relation

$$\frac{dE}{dt} = -D = -4vk^2E \quad (9.10)$$

we then obtain

$$t = -\frac{1}{4vk^2} \int \frac{dE}{E} = -\frac{1}{4vk^2} \int \frac{d\alpha_{max}}{\alpha_{max}} \quad (9.11)$$

and hence

$$\alpha_{max} \propto e^{-4vk^2t}. \quad (9.12)$$

In other words, the wave steepness in a low-amplitude solitary wave decays approximately twice as fast as in an infinite train of linear periodic waves. Evidently this is because, as the maximum steepness decays, the width of the solitary wave envelope increases, so that the decreasing total energy has to be distributed over a greater horizontal distance.

## 10. Discussion and comparison with experiment

The salient feature of figure 8 is the very sharp initial decreases in the surface slope  $\alpha_{max}$ , compared with the initial decrease for the pure capillary wave, as shown in figure 4. To understand this, we may first compare the rates of dissipation  $D$  for the two types of wave. The plots of  $D'$  and  $D$  in figures 3 and 6 cannot be compared directly since the physical scales are different. However, it is legitimate to compare the dimensionless quantities  $D/\mu q_0^2$  where  $q_0$  denotes the value of  $q$  in the central wave trough ( $\phi = 0$ ). For the pure capillary waves of §6 we have from equation (6.12)

$$q_0 = \left( \frac{1+A}{1-A} \right)^2 c \quad (10.1)$$

and so from (6.16)

$$\frac{D}{\mu q_0^2} = 64\pi \frac{A^6 + 4A^4 + A^2}{(1+A)^8} \quad (10.2)$$

where  $A = \tan(\alpha_{max}/4)$ . For the solitary waves  $D/\mu q_0^2$  can easily be found from the values of  $D/\mu$  and  $q_0$  given in table 1.

The numerical results are shown in figure 9, from which it is seen that the two curves follow one another very closely. This suggests that the sharp increase in dissipation at large  $\alpha_{max}$  is due in each case to the same cause, namely the large velocity gradients occurring in the troughs of each wave. In the wave troughs,  $q$  is large and the radius of curvature  $\kappa^{-1}$  is very small.

Note that since  $\kappa = d\alpha/ds$  equation (3.11), for example, can be written

$$\frac{D}{\mu c^2} = 2 \int_{-\infty}^{\infty} (q^2/c^2) d\alpha. \quad (10.3)$$

For very steep waves, the angle of slope  $\alpha$  goes rapidly from  $-\pi/2$  to  $+\pi/2$ . Thus the contribution to  $D/\mu c^2$  from the neighbourhood of the trough is of order  $2\pi q_0^2/c^2$ , which can become very large. In the rest of the integral where  $d\alpha$  is negative, the velocity  $q$  is much smaller, and so also is the contribution to the integral (10.3).

However the rate of decay of  $\alpha_{max}$  with time depends also on the energy density  $E$ , through its derivative  $dE/d\alpha_{max}$ . Here we can see obvious differences between the



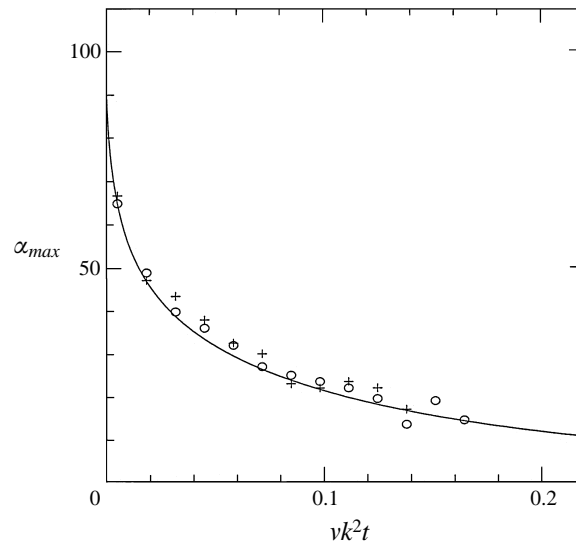


FIGURE 8. Time history of the maximum surface slope of a solitary wave decaying under viscosity. Curve: this paper; plotted points: experimental data (Longuet-Higgins & Zhang 1997).

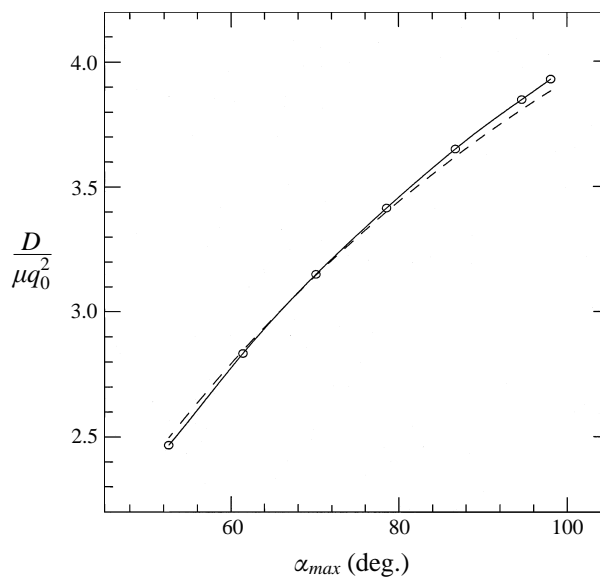


FIGURE 9. Comparison of the scaled dissipation  $D/\mu q_0^2$  in a solitary surface wave (plotted points) and in one wavelength of a pure capillary wave (dashed curve) as a function of the maximum surface slope  $\alpha_{max}$ .

solitary wave and the pure capillary wave. For the pure capillary wave  $E$  increases sharply at high values of  $\alpha_{max}$  (see figure 3). But for the solitary wave  $E$  increases only linearly (figure 7) and at high values of  $\alpha_{max}$  its rate of increase actually decreases. Physically this is because the gravitational part of the potential energy levels off and even decreases slightly as shown in figure 8 of Longuet-Higgins (1989). Again, this is due to the horizontal contraction of the solitary wave at high values of  $\alpha_{max}$ . Consequently the rate of decay of the solitary wave is much greater.

Finally in figure 8 we have plotted some experimental points representing the measured steepness of a freely decaying solitary wave as a function of the time  $t$ . In these experiments a solitary wave was excited by locally disturbing a uniform stream. The disturbance was then removed, and the solitary wave allowed to decay freely. For details, see Longuet-Higgins & Zhang (1997).

## 11. Conclusions

We have calculated the rates of viscous dissipation in two types of short surface waves: pure capillary waves and capillary gravity waves of solitary type on deep water. Both types of wave are assumed irrotational in the main body of the fluid, though not in surface boundary layers. In the pure capillary waves one can derive exact expressions for the energy dissipation, and hence for the instantaneous rate of decay of the wave amplitude. In the course of the decay, some vorticity will be spread from the surface boundary layer to the interior of the fluid. This vorticity is of second order in the wave steepness  $\alpha_{max}$  and if its interaction with the potential flow is neglected we may calculate the time history of the wave steepness as the wave decays. The result suggests that the steepness of pure capillary waves decreases at a nearly constant rate, over the whole range of wave amplitudes.

Similar calculations have been carried out for capillary gravity waves of solitary type. Here the methods used are essentially numerical, not analytic, but approximate formulae are available in two situations: when the surface slopes are very steep, and when they are small. When they are very steep, the numerical calculations, checked by the approximate formulae, indicate that at large values of the surface slope the dissipation increases very sharply, resulting in an exceptionally high rate of initial decay at large wave steepness.

When the solitary waves are low, they become essentially solitary wave 'packets' whose horizontal extent is inversely proportional to their maximum slope. Hence the limiting rate of decay of  $\alpha_{max}$  can be shown to be exactly twice that in an infinitely long wave of infinitesimal slope and comparable wavelength.

The theoretical rates of decay of solitary waves are in agreement with experiments on artificially generated solitary waves in the laboratory, at steepnesses  $\alpha_{max}$  less than  $50^\circ$  (see Longuet-Higgins & Zhang 1997). The very high theoretical rates of dissipation at larger values of  $\alpha_{max}$  may partly explain why very steep solitary waves are difficult to generate artificially.

This work has been supported by the US National Science Foundation under Grant OCE 93-14308 and the US Office of Naval Research under Contract N00014-94-1-0008.

## Appendix. Proof of equation (6.3)

Since in §6 the flow is to the right we have  $\alpha = \arg dz/d\phi$  and so from equation (6.11)

$$(\pi - \alpha) = \arg (\tan^2 w) = 2 \arg (\tan w). \quad (\text{A } 1)$$

But

$$\tan w = \tan (\phi + i\tau) = \frac{\tan \phi + i\tau}{1 - i\tau \tan \phi} \quad (\text{A } 2)$$

where

$$\tau = \tanh \psi = \frac{1-A}{1+A}. \quad (\text{A } 3)$$

From (A2)

$$\begin{aligned} \arg(\tan w) &= \tan^{-1}(\tau \cot \phi) + \tan^{-1}(\tau \tan \phi) \\ &= \tan^{-1} \frac{\tau(\cot \phi + \tan \phi)}{1 - \tau^2} \\ &= \tan^{-1} \left( \frac{2\tau}{1 - \tau^2} \operatorname{cosec} 2\phi \right). \end{aligned} \quad (\text{A } 4)$$

This has a minimum when  $\phi = \pi/4$  and  $\operatorname{cosec} 2\phi = 1$ . Hence

$$(\pi - \alpha_{\max}) = 2 \tan^{-1} \left( \frac{2\tau}{1 - \tau^2} \right) = 4 \tan^{-1} \tau. \quad (\text{A } 5)$$

Substituting from (A3) we have

$$(\alpha_{\max} - \pi) = 4 \tan^{-1} \frac{A-1}{A+1} = 4[\tan^{-1} A - \tan^{-1}(1)] = 4(\tan^{-1} A - \frac{1}{4}\pi). \quad (\text{A } 6)$$

This proves equation (6.3).

#### REFERENCES

- AKYLAS, T. R. 1993 Envelope solitons with stationary crests. *Phys. Fluids A* **5**, 789–791.
- CRAPPER, G. D. 1957 An exact solution for progressive capillary waves of arbitrary amplitude. *J. Fluid Mech.* **2**, 532–540.
- CRAPPER, G. D. 1970 Non-linear capillary waves generated by steep gravity waves. *J. Fluid Mech.* **40**, 149–159.
- DUBREIL-JACOTIN, M.-L. 1934 Sur la détermination rigoureuse des ondes permanentes périodiques d'amplitude finie. *J. Math. Pures Appliqués* **13**, 217–291.
- HOGAN, S. J. 1979 Some effects of surface tension on steep water waves. *J. Fluid Mech.* **91**, 167–180.
- LAMB, H. 1932 *Introduction to Hydrodynamics*, 6th edn. Cambridge University Press, 738 pp.
- LONGUET-HIGGINS, M. S. 1963 The generation of capillary waves by steep gravity waves. *J. Fluid Mech.* **16**, 238–159.
- LONGUET-HIGGINS, M. S. 1969 A non-linear mechanism for the generation of sea waves. *Proc. R. Soc. Lond. A* **311**, 371–389.
- LONGUET-HIGGINS, M. S. 1988 Limiting forms for capillary-gravity waves. *J. Fluid Mech.* **194**, 351–375.
- LONGUET-HIGGINS, M. S. 1989 Capillary-gravity waves of solitary type on deep water. *J. Fluid Mech.* **200**, 451–470.
- LONGUET-HIGGINS, M. S. 1992 Capillary rollers and bores. *J. Fluid Mech.* **240**, 659–679.
- LONGUET-HIGGINS, M. S. 1993 Capillary-gravity waves of solitary type and envelope solitons on deep water. *J. Fluid Mech.* **252**, 703–711.
- LONGUET-HIGGINS, M. S. & ZHANG, X. 1997 Laboratory experiments on capillary-gravity waves of solitary type in deep water. *Phys. Fluids* **9**, 1963–1968.
- VANDEN-BROECK, J.-M. & DIAS, F. 1992 Gravity-capillary solitary waves in water of infinite depth and related free-surface flows. *J. Fluid Mech.* **240**, 549–557.
- ZHANG, X. 1995 Capillary-gravity and capillary waves generated in a wind-wave tank: observations and theories. *J. Fluid Mech.* **289**, 51–82.